metals

MDPI

Supplementary Material for the Article

Batch Sintering of FeO·OH and Fe_2O_3 Blends: Chemical and Metallurgical Characterization

Igor J. U. V. Pereira [1], Henrique C. S. Coelho [1], Cláudio G. Santos [2], Eduardo A. Brocchi [3], Rodrigo F. M. Souza [3] and Victor A. A. Oliveira [1,*]

[1] Thermal Analysis and Non-Ferrous Extractive Metallurgy Laboratory, Department of Metallurgical and Materials Engineering, Universidade Federal de Ouro Preto, Ouro Preto 35400-000, MG, Brazil; igorjurandir@gmail.com (I.J.U.V.P.); henrique1990c@gmail.com (H.C.S.C.)
[2] Polymer Analysis Laboratory, Department of Chemistry, Universidade Federal de Ouro Preto, Ouro Preto 35400-000, MG, Brazil; claudio@ufop.edu.br
[3] Pyrometallurgy and Multiphysics Laboratory, Department of Chemical and Materials Engineering, Pontifícia Universidade Católica do Rio de Janeiro (PUC-Rio), Rio de Janeiro 22451-900, RJ, Brazil; ebrocchi@puc-rio.br (E.A.B.); rsouza@puc-rio.br (R.F.M.S.)
* Correspondence: victor@ufop.edu.br

i) X-ray diffractometry

The acquisition configuration of the equipment used to obtain the XRD is presented in table S1. Rietveld method was applied to determine the constituent minerals of the sample. To avoid potential issues that may arise from the mixing of an internal standard with the sample, the external standard method, also named G-method, was employed [1, 2]. This technique requires the recording of two patterns under identical diffractometer configuration and conditions [1].

Table S1. Acquisition configurations for the X-ray experiments.

Instrument	Malvern Panalytical Empyrean
Radiation	Cu Kα1,2
Geometry	Bragg-Brentano
Divergence slit	¼°
Generator	45kV, 40 mA
Mirror	BBHD®
Range	10 – 83°2θ
Step width	0.0131
Counting time	78.795 s
Detector	PIXcel1D-Medipix3
Rotation	1Hz

Silicon powder used in the external standard method was the well-known SRM 640f [3]. This material was used due to its high-purity. To compute scale factor without normalizing to 100 %, the factor K [4] shall be known, therefore Eq. (S1) [1] should be used.

$$K = s_{Si} \frac{\rho_{Si} V_{Si}^2 \mu_{Si}}{C_{Si}} \quad \text{(Eq. S1)}$$

where sSi is the Rietveld scale factor, ϱSi is the density, VSi is the unit-cell volume, CSi is the weight fraction, and μSi is the mass attenuation factor (MAC). The subscript Si signifies that the parameters refer to silicon. The models employed for the Rietveld refinement of each identified phase along with their corresponding ICDD codes are shown in Table S2.

Table S2. Models employed for the Rietveld refinement.

Phase	ICDD code	MAC (cm2/g)
Hematite	00-033-0664	220,77
Magnetite	00-019-0629	228,02
Quartz [5]	01-085-0795	34,84
Goethite [6]	01-084-8278	201,66
Kaolinite	00-058-2005	29,79
Dickite	00-058-2002	30,25
Chabazite-Mg [7]	04-017-9135	33,82

Copper radiation for iron containing materials leads to a high background due to fluorescence. To minimize this effect the pulse height distribution (PHD) was set to a range of 50-80%, this leads to increase in peak-to-noise ratio [8]. To achieve good particle statistics and minimize the microabsorption effects [9], the samples were milled in a vibratory disc mill with acetone, as this increases the efficiency of grinding [10], resulting in an approximate d50 value of 8 μm.

ii) Particle size of the raw materials

Table S3. Particle size distribution of the sample G_SF and H_SF.

Particle size (mm)	>6.3	> 1.0	>0.71	>0.3	>0.150	<0.150
G_SF (% wt.)	0	3.41	14.06	32.43	23.93	26.18
H_SF (% wt.)	7.43	22.66	16.43	17.11	16.34	20.03

Table S4. Particle size distribution of limestone and coke.

Limestone (mm)	> 5.6	> 3.0	> 1.0	> 0.21	< 0.21
Mass (% wt.)	0.0	10.8	23.1	27.3	38.8
Coque (mm)	> 5.0	> 3.0	> 1.0	> 0.21	< 0.21
Mass (% wt.)	3.5	2.6	63.6	21.4	8.7

iii) Sintering tests (Pilot scale)

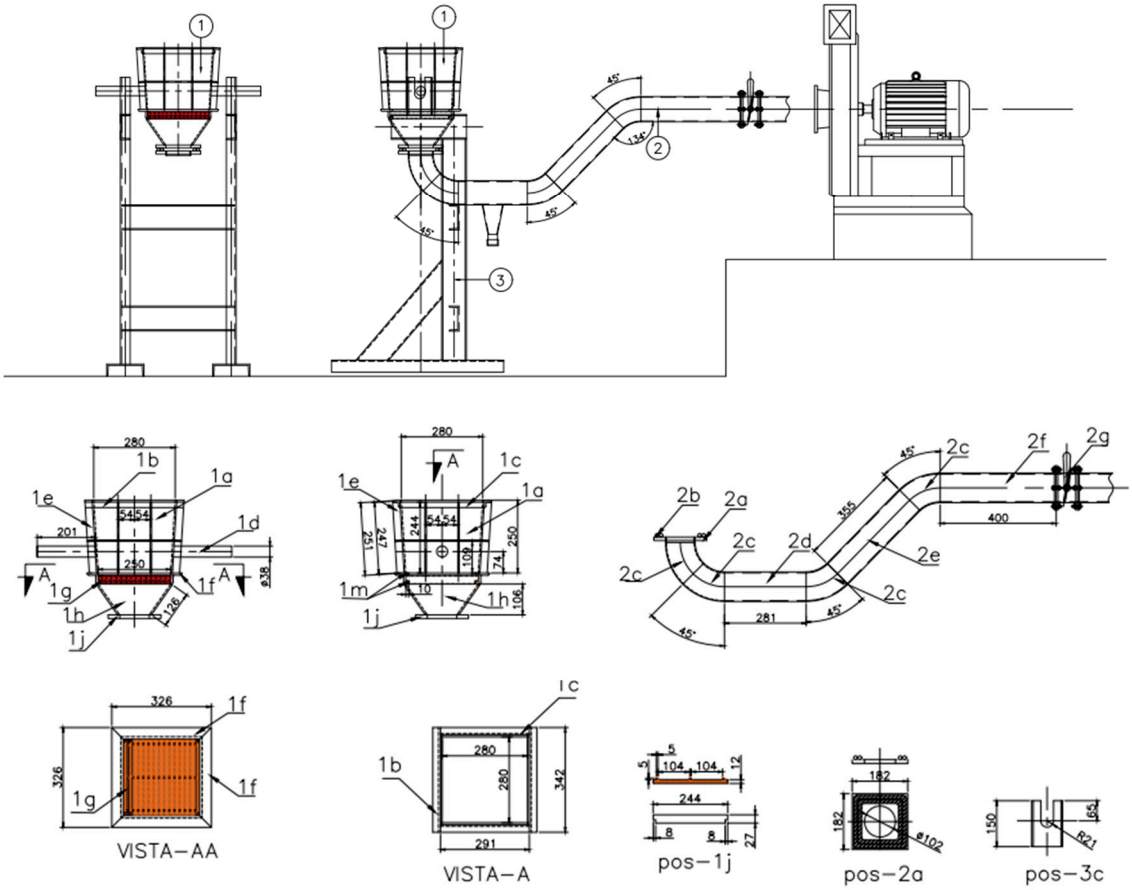

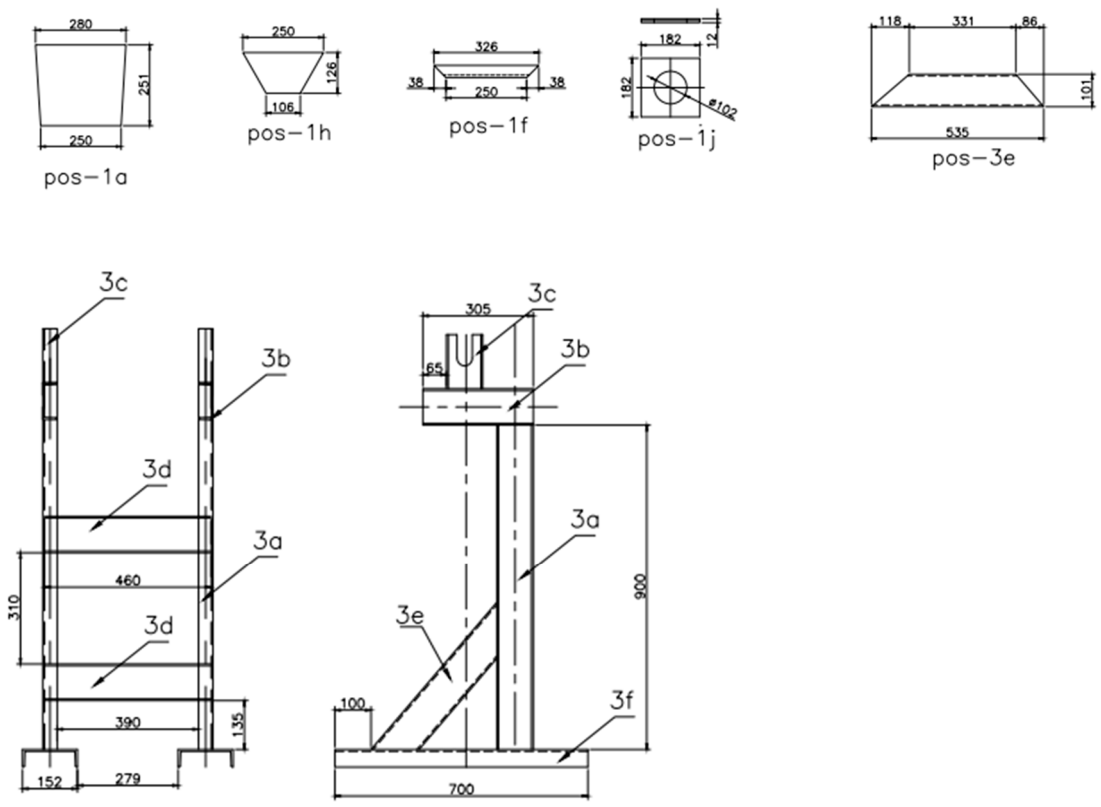

Figure S1. Dimensions (mm) and layout of the sinter plant.

Table S5. Specifications for the structural materials used in the sinter plant.

Reference	Quantity	Description	Material
1	4 sets		-
1a	4	Sheet 6.4 x 280 x 251 x 250	ASTM A36
1b	2	Angle 1″ x ¼ x 342	ASTM A36
1c	2	Angle 1″ x ¼ x 291	ASTM A36
1d	2	Round bar 1″1/2 x 200	ASTM A36
1e	8	Flat bar 1″1/2 x ¼ x 247	ASTM A36
1f	4	Angle 1″1/2 x 5/16 x 326	ASTM A36
1g	15	Sheet ½ x 244 x 27	ASTM A36
1h	4	Sheet 6.4 x 250 x 126 x 106	ASTM A36
1j	1	Sheet ½ x 182 x 182	ASTM A36
1m	4	Square bar 3/8 x 245	ASTM A36

2	1 pipe		
2a	1	Sheet ½ x 182 x 182	ASTM A36
2b	1	Red asbestos 1/2″ x 1500 mm	-
2c	4	Tube 45° 4″ DIN 2440	ASTM A36
2d	1	Tube 4″ x 291 DIN 2440	ASTM A36
2e	1	Tube 4″ x 355 DIN 2440	ASTM A36
2f	1	Tube 4″ x 400 DIN 2440	ASTM A36
2g	1	Butterfly valve 4″	ASTM A36
3	1 easel		
3a	2	Channel 4″ x 8.03 x 900	ASTM A36
3b	2	Channel 4″ x 8.03 x 305	ASTM A36
3c	2	Channel 4″ x 8.03 x 150	ASTM A36
3d	2	Channel 4″ x 8.03 x 460	ASTM A36
3e	2	Channel 4″ x 8.03 x 535	ASTM A36
3f	2	Channel 6″ x 12.2 x 700	ASTM A36

Figure S2. Sintering pilot plant

Figure S3. Bedding of granulated iron ore.

iv) Chemical analysis

Coke analysis

a) Moisture percentage

Pulverized coke (1.000 g) was dried at temperature of 150 °C for 12 minutes, and the percentage of mass loss during this process was determined as moisture content.

b) Determination of volatile material and fixed carbon

Dried pulverized coke (1.0000 g) was placed into a crucible, covered, and then subjected to a muffle furnace at a temperature of 950 °C for 1 hour. The percentage of mass loss during this process was determined as the volatile material, while the remaining mass in the crucible was attributed to fixed carbon.

c) Ash percentage

Dried pulverized coke (1.0000 g) was heated in a muffle furnace at 900 °C until a constant mass was achieved. The percentage of residual mass after burning was attributed to the ash percentage.

Table S6. Coke characterization.

Fixed carbon	Ash	Volatile matter	Moisture
78.4 %	6.7 %	9.5 %	5.4 %

Flux analysis

Table S7. Chemical composition of the limestone.

Fe	CaO	Mn	S	P	SiO2	Al2O3	MgO
3.7 %	56.0 %	0.1 %	0.07 %	0.12 %	2.5 %	1.0 %	1.0 %

Sintering bed analysis

Table S8. Chemical analysis of the mixes used as feed material in the sintering process.

	0%G_SF	10%G_SF	20%G_SF	30%G_SF	40%G_SF
SiO2 (%)	5.7	6.0	6.3	6.6	6.9
Fe (%)	53.9	53.4	52.9	52.4	51.9
Al2O3 (%)	1.3	1.4	1.6	1.7	1.8
Mn (%)	0.05	0.1	0.2	0.3	0.4
P (%)	0.04	0.05	0.05	0.05	0.05
S (%)	0.02	0.02	0.02	0.03	0.03
MgO (%)	0.10	0.09	0.09	0.09	0.08
K2O (%)	-	0.01	0.01	0.02	0.03
Cr2O3 (%)	0.28	0.28	0.27	0.26	0.25
TiO2 (%)	-	0.01	0.02	0.03	0.04
LOI (%)	2.4	2.9	3.3	3.8	4.2
Custo	X	0.93X	0.86X	0.79X	0.72X
Basicity	0.60	0.57	0.55	0.53	0.51
Slag (%)	16.29	16.97	17.66	18.34	19.02

Fixed carbon = 3.9%; CaO = 3.5 %.

v) Sinter characterization

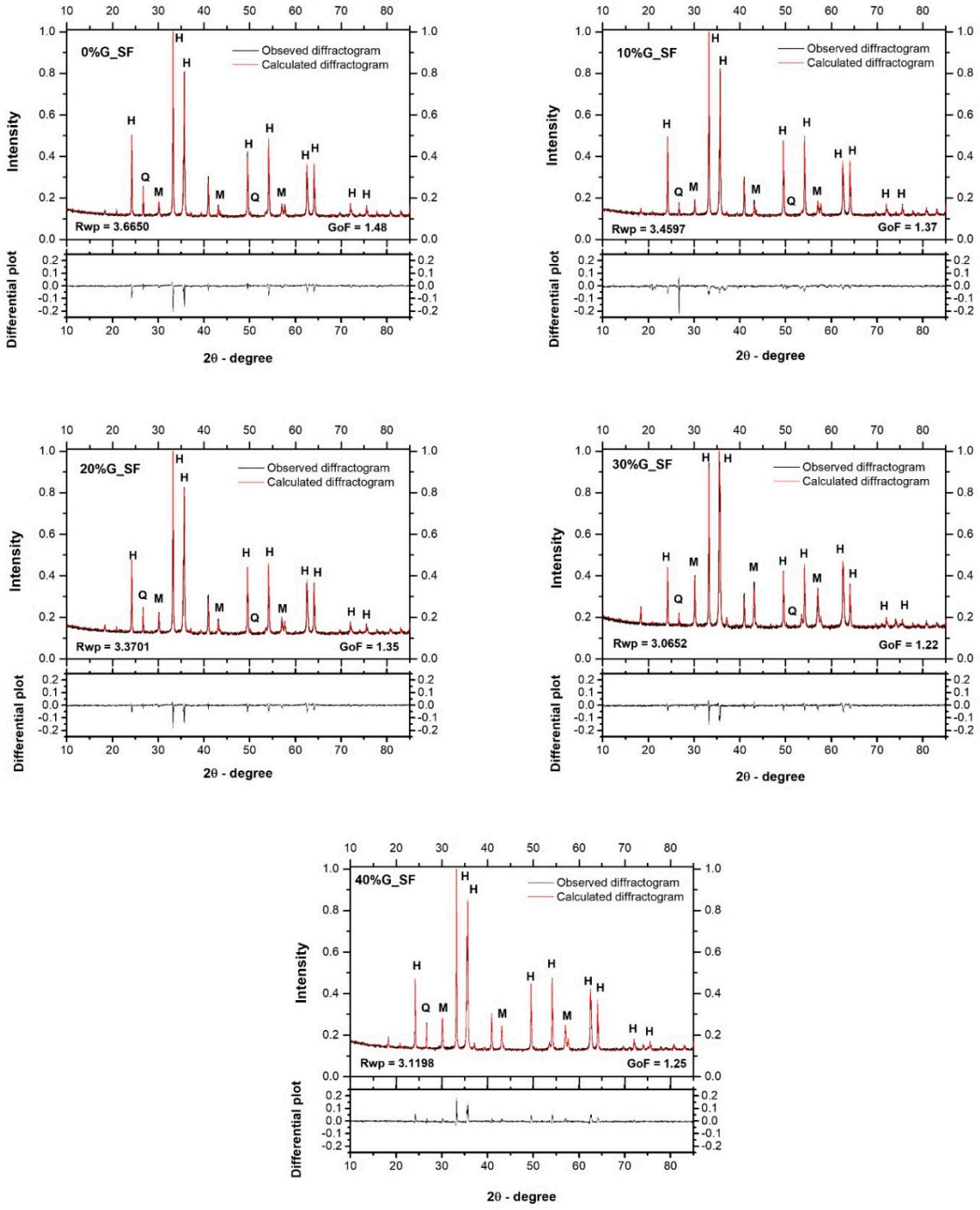

Figure S4. Observed and calculated diffractogram to the different sinters.

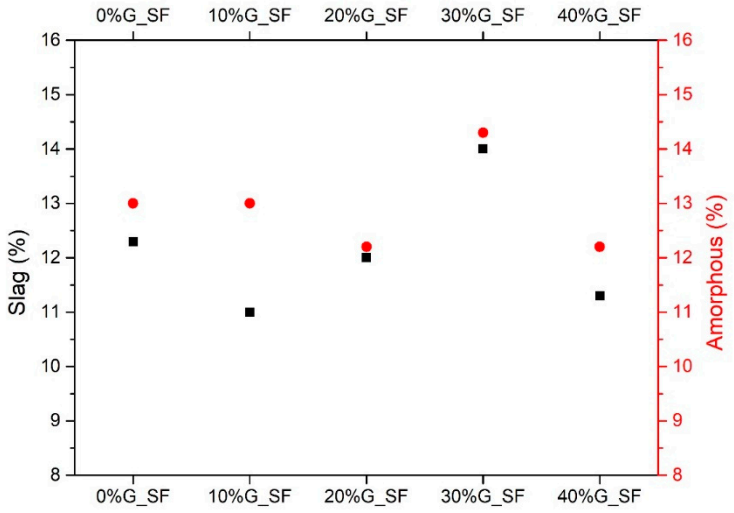

Figure S5. Correlation between the % of slag and the % of amorphous in the sinters.

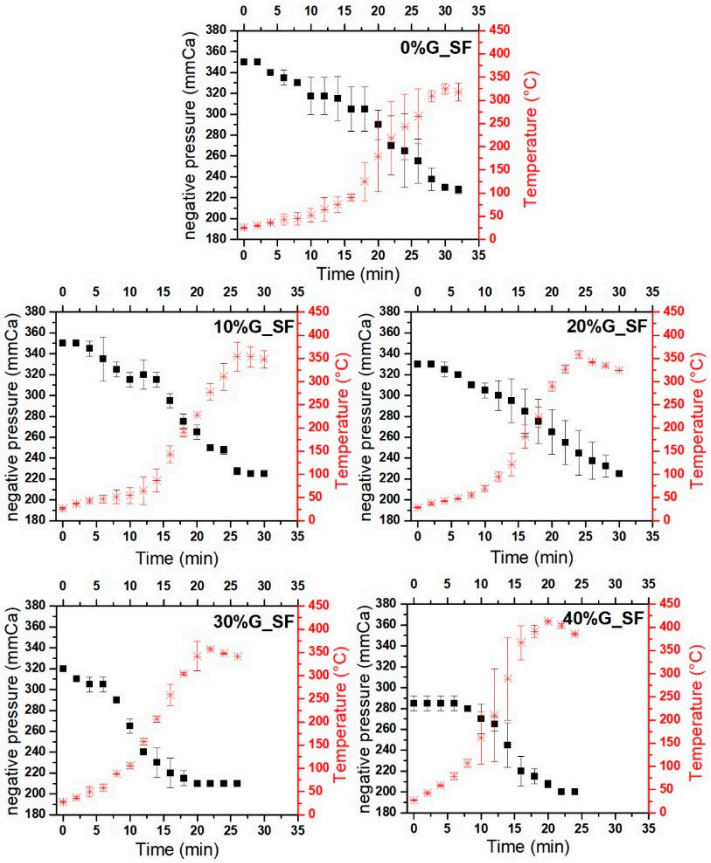

Figure S6. Sintering bed negative pressure and temperature of the gas at the windbox.

References in this supplementary document:

1. Dittrich, S., et al., Does Ordinary Portland Cement contain amorphous phase? A quantitative study using an external standard method. Powder Diffraction, 2011. 26(1): p. 31-38.
2. Aranda*, M.A.G., Á.G. De la Torre, and L. León-Reina, Rietveld Quantitative Phase Analysis of OPC Clinkers, Cements and Hydration Products. Reviews in Mineralogy and Geochemistry, 2012. 74(1): p. 169-209.
3. Black, D.R., et al., Certification of SRM 640f line position and line shape standard for powder diffraction. Powder Diffraction, 2020. 35(3): p. 156-159.
4. O'Connor, B.H. and M.D. Raven, Application of the Rietveld Refinement Procedure in Assaying Powdered Mixtures. Powder Diffraction, 1988. 3(1): p. 2-6.
5. Young, R.A., P.E. Mackie, and R.B. von Dreele, Application of the pattern-fitting structure-refinement method of X-ray powder diffractometer patterns. Journal of Applied Crystallography, 1977. 10(4): p. 262-269.
6. Zepeda-Alarcon, E., et al., Magnetic and nuclear structure of goethite ([alpha]-FeOOH): a neutron diffraction study. Journal of Applied Crystallography, 2014. 47(6): p. 1983-1991.
7. Montagna, G., et al., Chabazite-Mg: a new natural zeolite of the chabazite series. American Mineralogist, 2010. 95(7): p. 939-945.
8. Mos, Y.M., et al., X-Ray Diffraction of Iron Containing Samples: The Importance of a Suitable Configuration. Geomicrobiology Journal, 2018. 35(6): p. 511-517.
9. McCusker, L.B., et al., Rietveld refinement guidelines. Journal of Applied Crystallography, 1999. 32(1): p. 36-50.
10. Bish, D.L. and R.C. Reynolds, Sample preparation for X-ray diffraction. Reviews in Mineralogy and Geochemistry, 1989. 20(1): p. 73-99.